Side chain NMR assignments in the membrane protein OmpX reconstituted in DHPC micelles

Christian Hilty, César Fernández, Gerhard Wider & Kurt Wüthrich*
Institut für Molekularbiologie und Biophysik, Eidgenössische Technische Hochschule Zürich, CH-8093 Zürich, Switzerland

Abstract

Sequence-specific assignments have been obtained for side chain methyl resonances of Val, Leu and Ile in the outer membrane protein X (OmpX) from *Escherichia coli* reconstituted in 60 kDa micelles in aqueous solution. Using previously established techniques, OmpX was uniformly ^{2}H,^{13}C,^{15}N-labeled with selectively protonated Val-$\gamma^{1,2}$, Leu-$\delta^{1,2}$ and Ile-δ^1 methyl groups. The thus labeled protein was studied with the novel experiments 3D (H)C(CC)-TOCSY-(CO)-[^{15}N,^{1}H]-TROSY and 3D H(C)(CC)-TOCSY-(CO)-[^{15}N,^{1}H]-TROSY. Compared to the corresponding conventional experimental schemes, the TROSY-type experiments yielded a sensitivity gain of about 2 at 500 MHz. The overall sensitivity of the experiments was further enhanced more than two-fold by the use of a cryoprobe. Complete assignments of the proton and carbon chemical shifts were obtained for all isopropyl methyl groups of Val and Leu, as well as for the δ^1-methyls of Ile. The present approach is applicable for soluble proteins or micelle-reconstituted membrane proteins in structures with overall molecular weights up to about 100 kDa, and adds to the potentialities of solution NMR for *de novo* structure determination as well as for functional studies, such as ligand screening with proteins in large structures.

Abbreviations: 2D – 2-dimensional; 3D – 3-dimensional; CSA – chemical shift anisotropy; DHPC – dihexanoylphosphatidylcholine (1,2-dihexanoyl-*sn*-glycero-3-phosphocholine); HSQC – heteronuclear single quantum coherence; NOESY – nuclear Overhauser enhancement spectroscopy; OmpX – outer membrane protein X from *Escherichia coli*; ppm – parts per million; ST2-PT – single-transition-to-single-transition polarization transfer; TOCSY – total correlation spectroscopy; TROSY – transverse relaxation-optimized spectroscopy.

Introduction

During the past years, considerable efforts have been devoted to extend the application of solution NMR spectroscopy to larger molecular structures (for reviews, see Gardner and Kay, 1998; Riek et al., 2000; Wider and Wüthrich, 1999). With increasing molecular weight, rapid transverse spin relaxation causes line broadening and poor sensitivity, and the higher complexity of the NMR spectra results in increasing signal overlap. For studies of the polypeptide backbone, the problems arising from fast transverse spin relax-

ation in large structures have been largely overcome by combined use of protein deuteration (Gardner and Kay, 1998; LeMaster, 1994) and transverse relaxation-optimized NMR spectroscopy (TROSY) (Pervushin, 2000; Pervushin et al., 1997; Salzmann et al., 1998; Wider and Wüthrich, 1999; Wüthrich, 1998). As a result, sequence-specific backbone assignments have been obtained for polypeptide chains in structures of sizes up to 110 kDa (Salzmann et al., 2000). The potentialities of this approach are currently best exploited with systems that yield spectra of low complexity in spite of the large size, such as homo-oligomeric proteins (Salzmann et al., 2000), isotope-labeled membrane proteins reconstituted in unlabeled detergent mi-

A

^{1}H

y δ δ y — φ$_6$ — WALTZ — -y y — λ λ λ λ — φ$_{rec}$ — t_3 — i

^{13}C^{al} — φ$_2$ $t_1{}^a$ ε $t_1{}^b$ φ$_3$ $t_1{}^c$ SL — DIPSI-3 — a — b — c

^{13}C$^\alpha$ — ζ ζ η — SEDUCE-1

^{13}CO — SEDUCE-1 — φ$_4$ θ θ — d

^{15}N — φ$_5$ $T_N - \dfrac{t_2}{2} - \lambda$ $T_N + \dfrac{t_2}{2} - \lambda$ φ$_7$ — e — f — g — h

^{2}H — WALTZ-16

PFG — G$_1$ G$_1$ G$_2$ — G$_4$ G$_5$ G$_5$ G$_6$ — G$_7$ G$_7$ G$_8$ G$_8$

B

^{1}H

φ$_1$ φ$_2$ $t_1{}^a$ φ$_3$ $t_1{}^b$ $t_1{}^c$ y — φ$_6$ — -y WALTZ y — λ λ λ λ — φ$_{rec}$ — t_3 — i

^{13}C^{al} — ε ε SL — DIPSI-3 — a — b — c

^{13}C$^\alpha$ — ζ ζ η — SEDUCE-1

^{13}CO — SEDUCE — φ$_4$ θ θ — d

^{15}N — φ$_5$ $T_N - \dfrac{t_2}{2} - \lambda$ $T_N + \dfrac{t_2}{2} - \lambda$ φ$_7$ — e — f — g — h

^{2}H — WALTZ-16

PFG — G$_3$ G$_3$ G$_2$ G$_1$ G$_1$ — G$_4$ G$_5$ G$_5$ G$_6$ — G$_7$ G$_7$ G$_8$ G$_8$
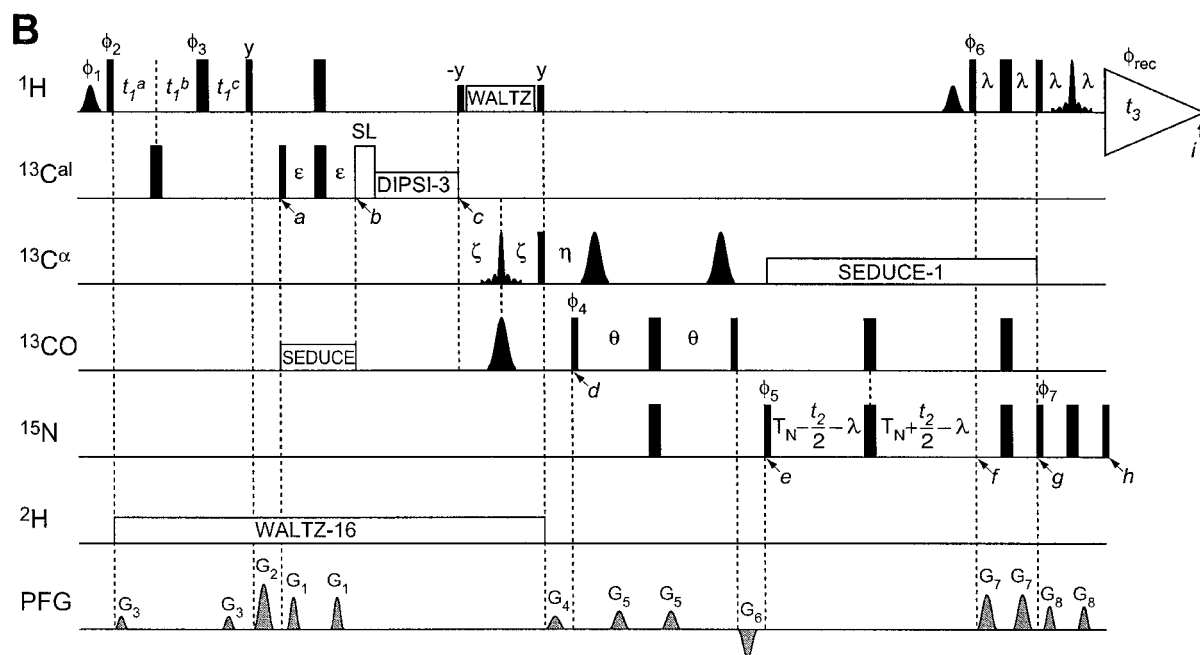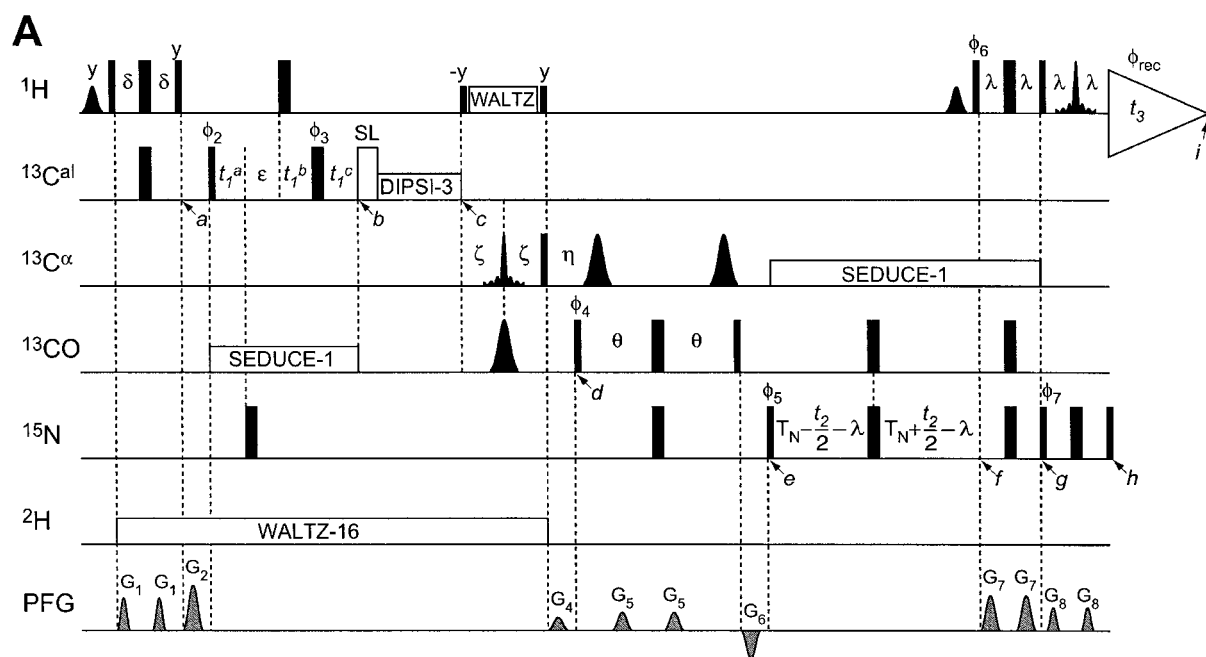
Figure 1. (A) Pulse sequence of 3D (H)C(CC)-TOCSY-(CO)-[^{15}N,^{1}H]-TROSY. (B) Pulse sequence of 3D H(C)(CC)-TOCSY-(CO)-[^{15}N,^{1}H]-TROSY. Rectangular 90° and 180° pulses are indicated by thin and thick black vertical bars, respectively, and phases are indicated above the pulses. Where no radio-frequency phase is marked, the pulse is applied along x. The ^{1}H carrier was placed at the position of the water line at 4.7 ppm, the ^{15}N carrier at 118 ppm, and the ^{13}C pulses were applied at ^{13}C^{al} = 38 ppm, ^{13}C$^{\alpha}$ = 56 ppm and ^{13}C′ = 175 ppm. The WALTZ-16 (^{1}H) sequence (Shaka et al., 1983) with a rf field strength of 3.3 kHz along the x-axis is used for ^{1}H decoupling of protein protons during the time period 2ζ; for work with perdeuterated proteins this element can be omitted, and it was not used in the work presented in this paper. Deuterium decoupling was achieved by a WALTZ-16 sequence with amplitude 0.7 kHz. The DIPSI-3 (Shaka et al., 1988) rf field amplitude for [^{13}C,^{13}C]-TOCSY was 10 kHz. ^{13}C$^{\alpha}$- and ^{13}C′-decoupling with SEDUCE-1 (McCoy and Mueller, 1992) was centered at 56 ppm with an amplitude of 1.67 kHz, and at 175 ppm with 0.83 kHz, respectively. The hard pulses on ^{13}C^{al}, ^{13}C$^{\alpha}$ and ^{13}C′ were applied with field strengths of 15 kHz, 4.4 kHz, and 3.9 kHz, respectively. The shaped 180°(^{13}C$^{\alpha}$) pulse between points *c* and *d* was a 1800 μs REBURP pulse selected to excite the region 54 ± 12 ppm. The 180°(^{13}C′) pulse between points *c* and *d* had a Gaussian profile with a truncation level of 5% and a duration of 300 μs, and was optimized to excite the carbonyl region at 175 ± 5 ppm. Because of off-resonance effects, the phase of the 90°(^{13}C$^{\alpha}$) pulse immediately preceding time point *d* has to be carefully adjusted to maximize the signal intensity. The two selective 180°(^{13}C$^{\alpha}$) pulses between time points *d* and *e* were applied with a Gaussian profile truncated at 5% and a duration of 150 μs, and were optimized to excite the region of 54 ± 12 ppm. The 180°(^{1}H) pulse before acquisition was optimized to suppress the DHPC signals, which are in the spectral region from 1 to 5 ppm, and the residual water signal using a REBURP pulse of duration 2866 μs for an excitation at 8.6 ± 3.5 ppm. The delays used were adjusted as follows: δ = 1/4^{1}J(C,H) = 1.7 ms, ε = 0.8 ms, ζ = 3.2 ms, θ = 11 ms, η = 4.5 ms; λ = 2.4 ms, T_N = 12.4 ms. The durations and amplitudes of the sine-bell-shaped pulsed field gradients were G_1 = 400 μs and 25 G/cm; G_2 = 800 μs and 35 G/cm; G_3 = 200 μs and 10 G/cm; G_4 = 800 μs and 10 G/cm; G_5 = 800 μs and 14 G/cm; G_6 = 800 μs and −22 G/cm, G_7 = 800 μs and 27 G/cm, and G_8 = 700 μs and 18 G/cm. The phase cycling was ϕ_1 = y; ϕ_2 = x; ϕ_3 = 8{x}, 8{−x}; ϕ_4 = 2{x}, 2{−x}; ϕ_5 = 2{y, −x}, 2{−y, x}; ϕ_6 = y; ϕ_7 = y; ϕ_{rec} = x,2{-x},x. Quadrature detection in t_1(^{13}C) (A) or t_1(^{1}H) (B) was accomplished by alternating the phases ϕ_2, or ϕ_1 and ϕ_2, respectively, according to States-TPPI (Marion et al., 1989). A phase-sensitive spectrum in the t_2(^{15}N) dimension was obtained by recording a second FID for each t_2 value, with ϕ_5 = 2{y, x}, 2{−y, −x}, ϕ_6 = −y and ϕ_7 = −y, and data processing as described by Kay et al. (1992). In (A), an additional phase cycle of the second 90°(^{1}H) pulse can be used to suppress peaks arising from ^{13}C steady-state magnetization (see text). The increments and delays for the ^{1}H and ^{13}C^{al} chemical shift evolution periods were set so as to achieve detection in a semi-constant-time manner (Grzesiek et al., 1993; Logan et al., 1993; Wider, 1998). In (A), the initial values for the delays during the t_1 evolution were t_1^a = t_1^b = 0, t_1^c = 1.05 ms, and in (B) t_1^a = t_1^c = 1.7 ms, t_1^b = 0. If no aliphatic resonances from detergents were to be suppressed, the last REBURP(^{1}H) pulse could be replaced by a WATERGATE sequence for improved water suppression. The 90° (^{1}H) water flipback pulses at the beginning of the pulse sequence and preceding time point *f* were applied for a duration of 1000 μs, using a Gaussian shape with a truncation level of 5%. For work with protein preparations containing protonated α-carbons, one may want to improve the selectivity of the first water flipback pulse by increasing its length.

celles (Arora et al., 2001; Fernández et al., 2001a,b), or labeled proteins in complexes with unlabeled nucleic acids.

Although uniform ^{2}H labeling enables solution NMR studies with large structures, it also limits the data collection to spin systems with labile protons, in particular the ^{15}N-^{1}H groups. In recent studies of the deuterated β-barrel membrane proteins OmpX (Fernández et al., 2001a,b) and OmpA (Arora et al., 2001; Fernández et al., 2001b) in micelles, the backbone fold could nonetheless be determined based on the experimental backbone H^N–H^N NOE distance constraints alone. Further refinement of the structures of OmpX and OmpA, and possibly other β-proteins requires supplementary data that have to be based on ^{1}H resonance assignments in amino acid side chains. For α-proteins, where only few long-range H^N–H^N NOEs can be expected (Wüthrich, 1986), even an initial fold determination will most probably require the assignment of side chain resonances.

In this paper, we describe new implementations of [^{15}N,^{1}H]-TROSY elements in experiments that correlate side-chain resonances with the backbone amide group in polypeptides, and thus enable the sequence-specific assignment for the corresponding side chain atoms. The 3D (H)C(CC)-TOCSY-(CO)-[^{15}N,^{1}H]-TROSY and 3D H(C)(CC)-TOCSY-(CO)-[^{15}N,^{1}H]-TROSY experiments have been applied with the integral membrane protein OmpX reconstituted in 60 kDa micelles, using a ^{2}H,^{13}C,^{15}N-labeled sample of OmpX in DHPC micelles with all Val-γ^{1,2}, Leu-δ^{1,2} and Ile-δ^1 methyl groups protonated (Goto et al., 1999). For a successful use of this approach, a high deuteration level has to be maintained to limit relaxation. Therefore, the coherence transfer from the periphery of the amino acid side chains to the α-carbons is *via* the carbon atoms, using [^{13}C,^{13}C]-TOCSY for efficient transfer of magnetization.

Materials and methods

Production of OmpX and NMR sample preparation

OmpX was overexpressed in *E. coli* BL21(DE3)pLysS cells harboring the plasmid pET3b-OmpX. For the preparation of selectively methyl-protonated and oth-

erwise uniformly ^{2}H,^{13}C,^{15}N-labeled OmpX, [u-^{2}H,^{13}C,^{15}N/L,V,Iδ^1-^{13}CH$_3$]-OmpX, transformed cells were first grown at 37 °C in 20 ml of Luria Bertani (LB) medium until the culture reached an optical density at 600 nm (OD$_{600}$) above 2.0. 3 ml of the LB culture were then used to inoculate 50 ml of unlabeled minimal medium (Hochuli et al., 2000), and the culture was grown at 37 °C. At OD$_{600}$ $\sim$ 0.5, the cells were spun down and transferred to 200 ml of minimal medium containing 99.9% D$_2$O, 4 g/l [^{13}C$_6$,^{2}H$_6$]-D-glucose ($> 98\%$ ^{13}C, $> 97\%$ ^{2}H) and 1 g/l ^{15}NH$_4$Cl ($> 98\%$ ^{15}N). When the culture reached again OD$_{600}$ $\sim$ 0.5, the cells were spun down and resuspended in 1 l of minimal medium with 99.9% D$_2$O, 4 g/l [^{13}C$_6$, ^{2}H$_6$]-D-glucose and 1 g/l ^{15}NH$_4$Cl. At OD$_{600}$ $\sim$ 0.3, 50 mg/l [3,3-^{2}H$_2$,^{13}C]-α-ketobutyrate and 100 mg/l [3-^{2}H, ^{13}C]-α-ketoisovalerate were added according to Goto et al. (1999). One hour later, protein overexpression was induced with 1 mM isopropyl-β-D-thiogalactopyranoside, and the cells were harvested by centrifugation once they had reached the stationary phase (approximately 4 h after induction). Protein isolation, purification, refolding and reconstitution into detergent micelles was performed as described previously (Fernández et al., 2001a). Finally, the sample was concentrated to a volume of 300 µl. The final sample conditions were: solvent H$_2$O; protein concentration, ~ 2 mM; buffer, 20 mM phosphate, 100 mM NaCl, 0.05% NaN$_3$, 200 mM DHPC, 5% ^{2}H$_2$O, pH = 6.8.

NMR pulse schemes for side-chain assignments

The 3D (H)C(CC)-TOCSY-(CO)-[^{15}N,^{1}H]-TROSY and the 3D H(C)(CC)-TOCSY-(CO)-[^{15}N,^{1}H]-TROSY experiments (Figure 1) correlate chemical shifts of the peripheral carbon atoms or protons of amino acid side chains with those of the backbone amide group of the following residue in the protein sequence. Based on the previously established assignment of the backbone amide group resonances, sequence-specific assignments of the side chain resonances can thus be obtained. The experimental schemes were derived by introducing the [^{15}N,^{1}H]-TROSY element into previously described experiments (Gardner et al., 1996; Grzesiek et al., 1993; Lin and Wagner, 1999; Logan et al., 1993; Lyons and Montelione, 1993; Lyons et al., 1993; Montelione et al., 1992).

In the experiment of Figure 1A, which correlates the methyl ^{13}C spins with the ^{15}N-^{1}H groups, proton magnetization generated by the first non-selective 90° pulse is transferred to the directly attached carbon using an INEPT step. With the presently used selective protonation of methyl groups, this transfer is limited to peripheral methyls. Between time points *a* and *b*, magnetization of the protonated methyl carbons (^{13}C^{al}) evolves during a semi-constant time evolution period (Grzesiek et al., 1993; Logan et al., 1993; Wider, 1998) and the methyl carbon spins are refocused to in-phase coherence with respect to the methyl protons. With [^{13}C,^{13}C]-TOCSY using a DIPSI-3 mixing sequence (Bax et al., 1990; Shaka et al., 1988; Wider, 1998), a fraction of the methyl ^{13}C magnetization (^{13}C^{al} in Figure 1) is transferred to the α-carbons of the same residue (time point *c*). Between time points *c* and *d*, this magnetization is transferred intraresidually to the carbonyl carbons, whereby two selective pulses applied simultaneously on ^{13}C$^\alpha$ and ^{13}C$'$ refocus the $^1J(\text{C}^\alpha, \text{C}^\beta)$ coupling. Between time points *d* and *e*, magnetization is transferred from ^{13}C$'$ to the nitrogen of the sequentially following amino acid residue, where two selective pulses applied on ^{13}C$^\alpha$ generate in-phase ^{13}C$'$ coherence with respect to ^{13}C$^\alpha$. Between time points *e* and *g*, ^{15}N magnetization evolves during a constant-time evolution period. This time period is concatenated with the TROSY ST2-PT element (Pervushin et al., 1998; Salzmann et al., 1999). [^{15}N,^{1}H]-TROSY coherence transfer from the nitrogen to the amide proton takes place between the time points *f* and *h*. The last 180° (^{1}H) pulse was applied selectively to the amide proton spectral region, thus suppressing the ^{1}H signals from the highly abundant detergent molecules in the spectral region upfield of 5 ppm. Instead of using a selective pulse, the TROSY element could be combined with gradient selection (Pervushin et al., 1997). However, this would require exact calibration of the gradients and interruption of the SEDUCE decoupling sequence on C$^\alpha$, and therefore we gave preference to the scheme of Figure 1.

The experiment of Figure 1B, which correlates the methyl protons with the ^{15}N-^{1}H groups, differs from the scheme in Figure 1A in that ^{1}H magnetization is transferred to ^{13}C^{al} before time point *b*, using a semi-constant time evolution on protons. Between time points *a* and *b*, the ^{13}C^{al} anti-phase coherence is converted to in-phase carbon magnetization with respect to protons. In both schemes, two selective pulses on the water resonance ensure that the water magnetization stays along the +z axis most of the time. Furthermore, two 90° (^{1}H) pulses flanking the

WALTZ proton decoupling sequence are used to ensure that the water magnetization is in a spin-locked state, and thus to minimize loss of coherence during the proton decoupling.

NMR experiments with OmpX/DHPC

The NMR experiments were recorded at 30 °C on a Bruker DRX-500 spectrometer equipped with four radio-frequency channels for generating the ^{1}H, ^{2}H, ^{13}C and ^{15}N pulses, and a ^{1}H-{^{13}C,^{15}N}-triple resonance cryoprobe with an actively shielded z-gradient coil (Wider, 1998). The following parameters were used: 3D (H)C(CC)-TOCSY-(CO)-[^{15}N,^{1}H]-TROSY: time domain data size 50(t_1) × 26(t_2) × 512(t_3) complex points, $t_{1\,max}$(^{13}C) = 5.0 ms, $t_{2\,max}$(^{15}N) = 17.1 ms, $t_{3\,max}$(^{1}H^N) = 64.0 ms, digital spectral resolution, 39 Hz (^{13}C), 12 Hz (^{15}N) and 8 Hz (^{1}H^N), spectral size 256(t_1) × 128(t_2) × 1024(t_3); 3D H(C)(CC)-TOCSY-(CO)-[^{15}N,^{1}H]-TROSY: data size 50(t_1) × 26(t_2) × 512(t_3) complex points, $t_{1\,max}$(^{1}H) = 16.6 ms, $t_{2\,max}$(^{15}N) = 17.1 ms, $t_{3\,max}$(^{1}H^N) = 64.0 ms, digital spectral resolution, 16 Hz (^{1}H), 12 Hz (^{15}N) and 8 Hz (^{1}H^N), spectral size 256(t_1) × 128(t_2) × 1024(t_3). For both spectra, 64 transients were recorded per FID, with a total measuring time of about 4 days. This would correspond to at least 16 days, if no cryoprobe were available. A 2D [^{13}C,^{1}H]-COSY experiment (Bodenhausen and Ruben, 1980) was measured at 30 °C on a Bruker DRX-800 spectrometer. The data size was 160 (t_1) × 1024 (t_2) complex points, $t_{1\,max}$(^{13}C) = 11.4 ms, $t_{2\,max}$(^{1}H) = 91.8 ms, digital spectral resolution, 27 Hz (^{13}C) and 11 Hz (^{1}H), spectral size 512(t_1) × 2048(t_2). 16 transients were recorded per FID. Chemical shifts were referenced to a standard of 2,2-dimethyl-2 silapentane-5-sulfonate sodium salt (DSS) (Markley et al., 1998).

Results

In the 2D [^{1}H,^{13}C]-COSY spectrum of the sample with selective methyl protonation, [u-^{2}H,^{13}C,^{15}N/L,V, Iδ^1-^{13}CH$_3$]-OmpX/DHPC, correlation peaks are readily detectable in the region containing methyl resonances (Figure 2A) but otherwise an empty spectrum was obtained (data not shown). This indicates that the deuteration level of the remaining CH$_n$ groups of the protein is close to 100%. 3D (H)C(CC)-TOCSY-(CO)-[^{15}N,^{1}H]-TROSY and 3D H(C)(CC)-TOCSY-(CO)-[^{15}N,^{1}H]-TROSY experiments with this preparation

Table 1. Methyl ^{1}H and ^{13}C chemical shifts of OmpX/DHPC at pH = 6.5 and T = 30 °C, measured in selectively methyl-protonated and otherwise uniformly ^{2}H,^{13}C,^{15}N-labeled OmpX reconstituted in DHPC micelles, [u-^{2}H,^{13}C,^{15}N/L,V, Iδ^1-^{13}CH$_3$]-OmpX/DHPC

Methyl groups	Chemical shifts[a]
Val 5	21.0 (0.98), 21.5 (1.06)
Leu 26	24.5 (0.95), 25.8 (0.90)
Leu 37	24.4 (1.03), 25.4 (0.96)
Val 39	20.5 (0.87), 21.1 (0.88)
Ile 40 δ^1	14.4 (−0.49)
Ile 65 δ^1	14.1 (0.82)
Ile 73 δ^1	13.5 (0.65)
Ile 79 δ^1	14.0 (0.69)
Val 82	17.0 (0.36), 22.6 (0.41)
Val 83	19.1 (1.02), 22.2 (1.11)
Val 85	21.1 (0.95), 21.1 (0.99)
Leu 113	24.3 (0.74), 26.0 (0.77)
Val 121	21.3 (0.93), 21.4 (0.98)
Leu 123	23.8 (0.98), 25.6 (0.96)
Ile 132 δ^1	11.7 (0.61)
Val 135	20.8 (0.32), 20.8 (0.64)
Val 137	19.9 (−0.05), 20.5 (0.43)
Ile 141 δ^1	14.3 (0.27)
Val 144	19.7 (0.91), 21.1 (0.92)

[a]The chemical shifts are in ppm relative to internal 2,2-dimethyl-2 silapentane-5-sulfonate sodium salt (DSS). The first number is the ^{13}C shift, and the corresponding ^{1}H shift is given in parentheses. The diastereotopic isopropyl methyl resonances (Neri et al., 1990) of Val and Leu have not been individually assigned.

were measured on a 500 MHz Bruker Avance spectrometer equipped with a cryoprobe, to correlate side chain methyl resonances with previously assigned resonances of the backbone amide groups. Strips from the two spectra corresponding to the selectively protonated amino acids (Figures 2B and C) contain peaks correlating the methyl ^{13}C (Figure 2B) or the methyl ^{1}H (Figure 2C) chemical shifts with the ^{15}N and ^{1}H chemical shifts of the sequentially following amino acid residue. As a result of the combined analysis of the two spectra, sequence-specific assignments of all the proton and carbon resonances of the protonated methyl groups could be obtained (Table 1).

A comparison of the new TROSY experiments (Figure 1) with otherwise identical conventional experiments (Lin and Wagner, 1999) for OmpX reconstituted in DHPC micelles revealed sensitivity gains of up to a factor of 2.5 for the individual cross peaks (Figure 3). In this comparison, a conventional
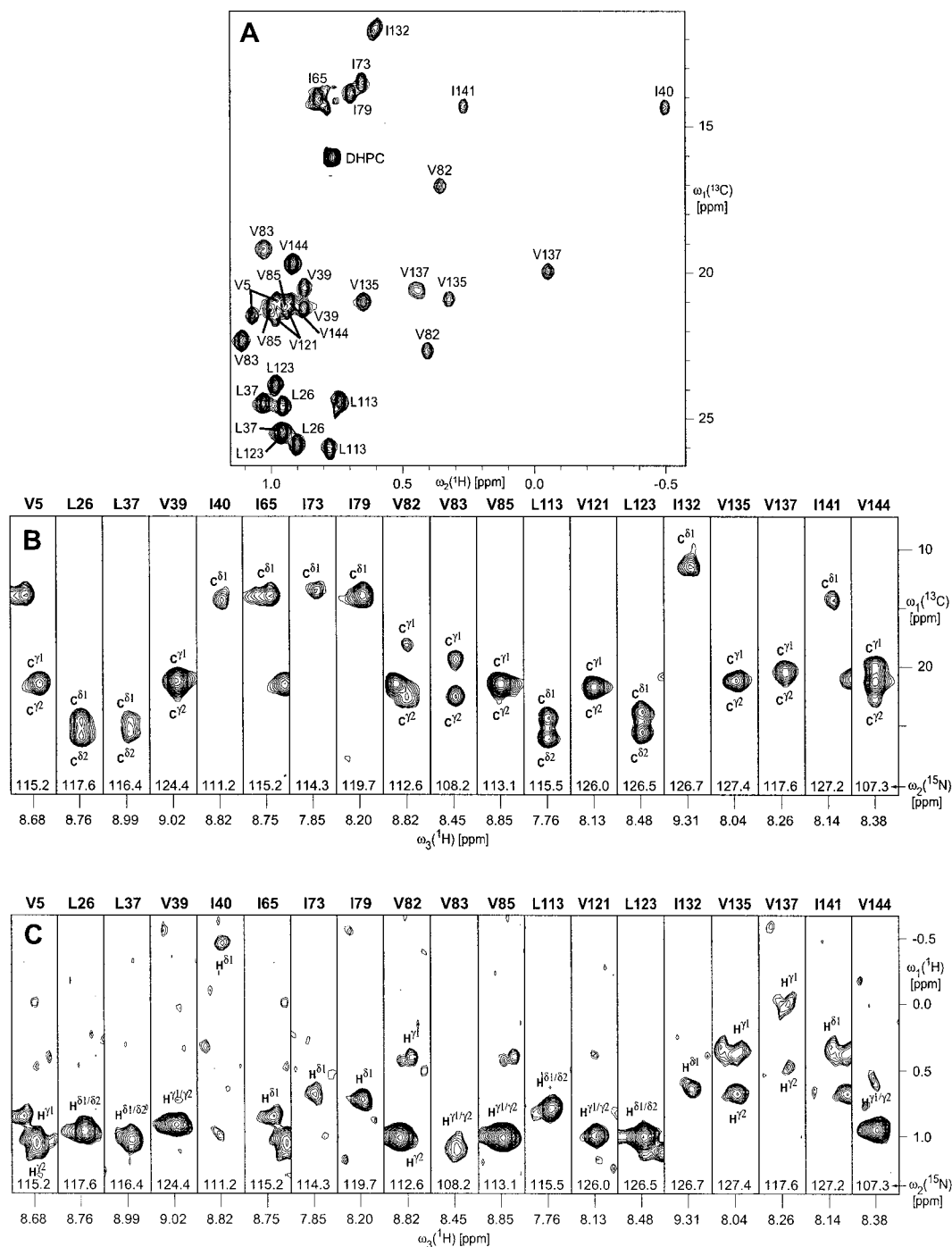
294

Figure 2. (A) 2D [^{1}H,^{13}C]-COSY spectrum showing the Val-$\gamma^{1,2}$, Leu-$\delta^{1,2}$ and Ile-δ^1 methyl resonances of [u-^{2}H,^{13}C,^{15}N/L,V,Iδ^1-^{13}CH$_3$]-OmpX/DHPC measured on a Bruker DRX-800 spectrometer (digital spectral resolution 27 Hz (^{13}C) and 11 Hz (^{1}H)). The strong signal labeled DHPC arises from the natural abundance of ^{13}C in the detergent, which is present in the sample at a concentration of 200 mM. (B) [ω_1(^{13}C), ω_3(^{1}H)]-strips from the 3D (H)C(CC)-TOCSY-(CO)-[^{15}N,^{1}H]-TROSY spectrum (digital spectral resolution 39 Hz (^{13}C), 12 Hz (^{15}N) and 8 Hz (^{1}H^N)). (C) [ω_1(^{1}H), ω_3(^{1}H)]-strips from the 3D H(C)(CC)-TOCSY-(CO)-[^{15}N,^{1}H]-TROSY spectrum (digital spectral resolution 16 Hz (^{1}H), 12 Hz (^{15}N) and 8 Hz (^{1}H^N)). The strips were taken at the ^{15}N chemical shifts indicated at the bottom and are centred about the ω_3(H^N) chemical shifts of the amino acid residues following the Val, Leu and Ile residues indicated at the top of the strips. The methyl ^{13}C or ^{1}H chemical shifts of the residues indicated at the top of the strips were measured along ω_1. Both spectra were acquired on a Bruker DRX-500 spectrometer equipped with a triple-resonance cryoprobe. The following sample conditions were used for all three spectra: 2 mM solution of [u-^{2}H,^{13}C,^{15}N/L,V,Iδ^1-^{13}CH$_3$]-OmpX/DHPC, solvent H$_2$O, 20 mM phosphate, 100 mM NaCl, 0.05% NaN$_3$, 200 mM DHPC, 5% ^{2}H$_2$O, pH = 6.8, T = 30 °C.
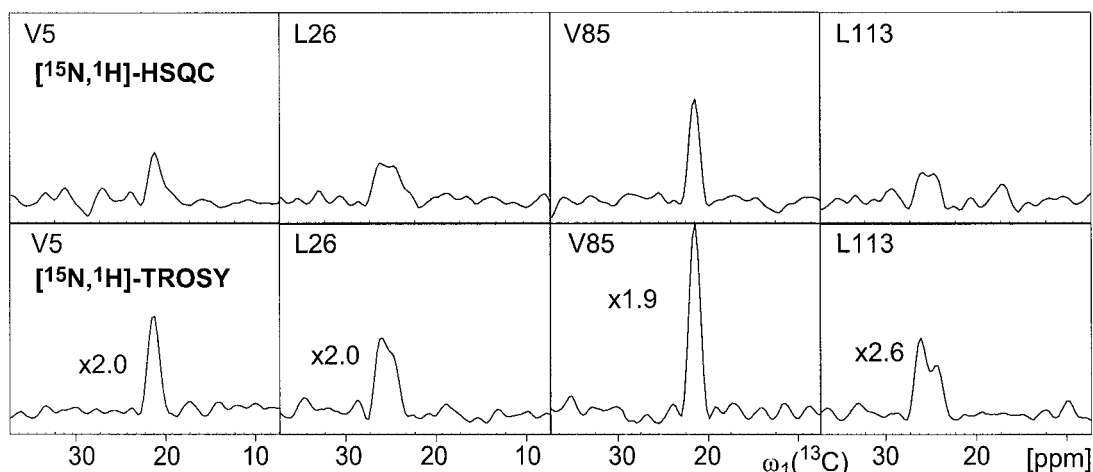
Figure 3. Comparison of data obtained with and without a [^{15}N,^{1}H]-TROSY element in the (H)C(CC)-TOCSY-(CO)-NH experiment at 500 MHz. Slices were taken along the carbon frequency through the maxima of the peaks that were, as a result of these experiments, assigned to the residues indicated in the Figure with the one-letter amino acid symbol and the sequence number. The sensitivity gain observed for the TROSY experiment is indicated with the bottom traces. The experimental conditions are described in Figure 2 and in the text, the measuring time for each spectrum was 22 h.

HSQC transfer was used, since for large molecules the gain from an additional coherence transfer step in sensitivity-enhanced schemes is smaller than the losses due to the additional relaxation during the longer experiment.

Discussion

Selection of the field strength

Three key factors for deciding on the optimal ^{1}H resonance frequency for the experiments yielding side chain assignments were considered, i.e., the field dependence of the [^{15}N,^{1}H]-TROSY effect with a maximum near 1000 MHz (Wüthrich, 1998), the increased transverse relaxation at higher fields due to the large CSA of the carbonyl ^{13}C, and the fact that a cryoprobe was available to us at 500 MHz. The field dependence of the sensitivity was estimated from calculations considering transverse spin relaxation due to dipole-dipole interactions and CSA with and without use of TROSY, as well as the INEPT polarization transfer efficiencies (Salzmann et al., 1998).

The B_0 dependence of the sensitivity, S_{rel}, for the experiment of Figure 1A was calculated from time point c onwards as described in the Appendix. The computations were performed for a β-sheet in a protein with a rotational correlation time of 21 ns, which corresponds to the OmpX/DHPC molecular size of about 60 kDa. The values for the parameters used are given in the legend to Figure 4.

The plots of the field dependence of the expected signal intensities (Figure 4A) suggest that the sensitivity of (H)C(CC)-TOCSY-(CO)-[^{15}N,^{1}H]-TROSY reaches a maximum at a proton resonance frequency of 500–600 MHz (dashed lines in Figure 4A). Because the large chemical shift anisotropy of the carbonyl group significantly contributes to the T_2 relaxation rate at higher fields (Loria et al., 1999; Permi and Annila, 2001), the overall sensitivity decreases rapidly for increasing field strength. Measurements at 500 MHz were then an obvious choice, given that a cryoprobe was available at this field, boosting the intrinsic spectrometer sensitivity to a level that is comparable to that of a 800 or 900 MHz spectrometer equipped with a conventional probehead. Furthermore, at 500 MHz efficient [^{13}C,^{13}C]-TOCSY mixing of the aliphatic carbons in the amino acid side chains is more readily achieved and produces less heating than at higher field. Overall, the calculation predicts a nearly 3-fold gain for the TROSY-type experiment at 500 MHz (broken lines in Figure 4A) when compared to the conventional experiment (solid lines in Figure 4A). The spread indicated for both versions of the experiment by the gray areas reflects the range of values observed in globular proteins for the scalar coupling constants that determine the INEPT transfer efficiency. The predictions from these model calculations seem to be confirmed by the experimental data, which show TROSY en-
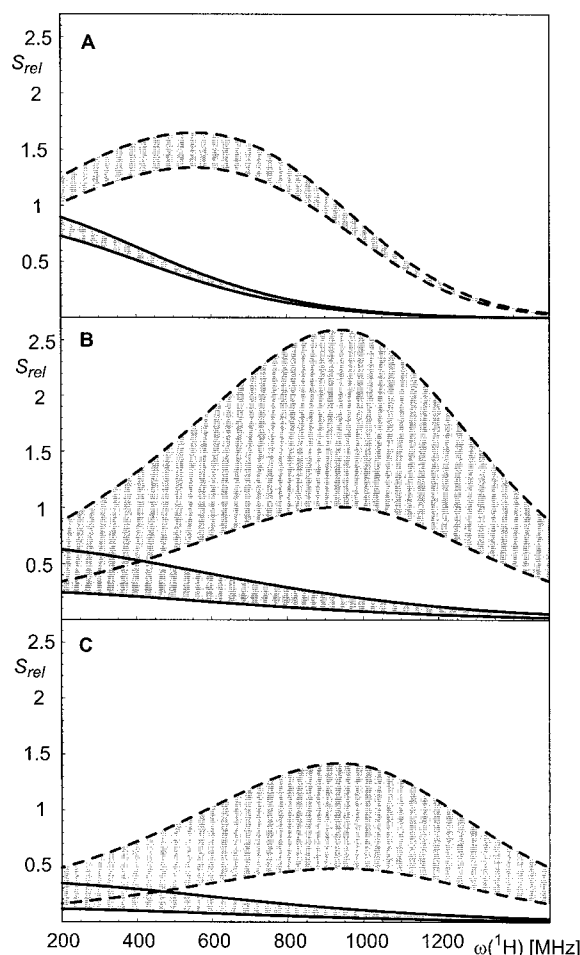
Figure 4. Frequency dependence of the relative signal intensities, S_{rel}, achievable with the pulse sequences of Figures 1A and 6, computed using the formalism of Appendix A. The computations considered transverse relaxation due to dipole-dipole and CSA interactions, and the J-coupling-dependent transfer functions were computed for the upper and lower limit values of the coupling constants observed in globular proteins (for details see the Appendix). The resulting spread of the overall signal intensities is given by the areas with gray shading. (A) (H)C(CC)-TOCSY-(CO)-[^{15}N,^{1}H]-TROSY experiment (dashed lines) and the conventional counterpart (solid lines), calculated from time point c onward (Figure 1A). (B) Intraresidual peak in (H)C(CC)-TOCSY-[^{15}N,^{1}H]-TROSY (dashed lines) and its conventional counterpart (solid lines). (C) Sequential peak in (H)C(CC)-TOCSY-[^{15}N,^{1}H]-TROSY (dashed lines) and its conventional counterpart (solid lines). The calculations are for an antiparallel β-sheet in a protein with an effective rotational correlation time of 21 ns. The following parameters were used: amide nitrogen CSA, $\Delta\sigma_N = -157$ ppm, $\varphi_N = 15.7°$ (φ_N is the angle between the principal axis of the axially symmetric CSA tensor and the chemical bond linking H^N and N); amide proton CSA, $\Delta\sigma_H = 13$ ppm, $\varphi_H = 10.0°$; carbonyl carbon CSA, $\Delta\sigma_{C'} = -125$ ppm; C$^\alpha$ CSA, $\Delta\sigma_{C\alpha} = 25$ ppm; $^{2}J(C^\alpha,N) = 6$–9 Hz; $^{1}J(N,C^\alpha) = 7$–11 Hz; $^{1}J(C',N) = 13$–15 Hz; $^{1}J(C^\alpha,C') = 53$–56 Hz; distances between dipole-dipole-coupled atoms: $r(N–H) = 1.04$ Å, $r((NH)_i–(NH)_{i+1}) = 4.3$ Å, $r((NH)_i–(NH)_j)$ [across the β-sheet] $= 3.3$ Å (Wüthrich, 1986). The delays between time points k and l in Figure 1A, t_{kl}, were taken directly from the experiment. For the TROSY-type (Figure 6A) and the conventional (H)C(CC)-TOCSY-NH experiments, $t_{de} = 26.4$ ms. For the remaining delays and parameters, identical values to those in the (H)C(CC)-TOCSY-(CO)-[^{15}N,^{1}H]-TROSY experiment of Figure 1A were used.

hancements of up to about 2.5, depending on the residue (Figure 3).

Variations of the pulse sequences

Depending on the system studied, the pulse sequences for the (H)C(CC)-TOCSY-(CO)-[^{15}N,^{1}H]-TROSY and the H(C)(CC)-TOCSY-(CO)-[^{15}N,^{1}H]-TROSY experiments may be slightly varied from the versions in Figure 1. The following modifications may be of practical interest: (i) The ^{1}H WALTZ decoupling element between time points c and d is not needed when the C$^\alpha$ positions are completely deuterated, as was the case in this study. Omitting this decoupling

period results in an increase of the extent to which the water magnetization can be flipped back, and reduces sample heating. (ii) The last proton pulse was implemented as a selective 180° REBURP pulse (Geen and Freeman, 1991) centered on the amide protons. This pulse leaves the water magnetization along the z-axis, and the flanking G_8 gradients suppress the residual water line as well as signals from the aliphatic protons of the protonated detergent. For samples that do not contain high proton concentrations from unlabeled molecules, this pulse can be replaced by a WATER-GATE element (Piotto et al., 1992; Salzmann et al., 1998). (iii) ^{2}H decoupling can be omitted for non-deuterated proteins. (iv) For very large structures, the ST2-PT element (Figure 1, between time points f and h) can be replaced by a normal INEPT transfer, or omitted altogether to reduce the overall duration of the experiment and thus to reduce relaxation losses. The resulting experiment yields four-component multiplets typical of undecoupled COSY spectra (Pervushin et al., 1997). However, for large particles with very long τ_c, the line widths of the four components differ so strongly that only the most slowly relaxing line is observable, which corresponds to the 'TROSY component' selected by the ST2-PT element.

Extra peaks arising from ^{13}C steady-state magnetization

In the 3D (H)C(CC)-TOCSY-(CO)-[^{15}N,^{1}H]-TROSY experiment, steady-state magnetization of non-protonated carbons can give rise to extra peaks in the spectrum. These peaks may be useful for obtaining additional ^{13}C assignments, may help to find the resonance positions of individual amino acid residues in the 3D spectrum, and may also give information on the type of the amino acid. In [u-^{2}H,^{13}C,^{15}N/L,V,Iδ^1-^{13}CH$_3$]-OmpX/DHPC such resonances were observed for the majority of the residues (Figure 5). In spite of their potentially interesting information content, one may want to suppress these additional resonances in order to simplify the spectra. This can be achieved either by inverting the phases of the first hard ^{1}H pulse, the preceding shaped pulse and of the receiver (Figure 1A), or by applying a 90°(^{13}C^α) pulse followed by a pulsed field gradient at the end of the recycle delay.

Comparison with the (H)C(CC)-TOCSY-[^{15}N,^{1}H]-TROSY experiment

At higher field strengths, direct magnetization transfer from C^α to both neighboring nitrogens appears *a*

priori to be an attractive alternative to the (H)C(CC)-TOCSY-(CO)-[^{15}N,^{1}H]-TROSY experiment. Both the sequential and the intraresidual side-chain resonances could thus be correlated with the ^{1}H and ^{15}N chemical shifts.

Since in this experiment the carbonyl ^{13}C CSA does not contribute to the transverse relaxation of the signals of interest, the optimal sensitivity for the TROSY version of the experiment (Figure 6) is expected at around 900–1000 MHz (Figures 4B and C). The calculations of the Appendix further suggest that the (H)C(CC)-TOCSY-[^{15}N,^{1}H]-TROSY experiment at 800 MHz should have comparable sensitivity to the (H)C(CC)-TOCSY-(CO)-[^{15}N,^{1}H]-TROSY experiment at 500 MHz, since the two spectrometers have similar intrinsic sensitivities due to the use of a conventional probehead and a cryogenic probehead, respectively, and that up to time point c (Figures 1 and 6) the experiment is independent of B_0. In the practice of our experiments, however, the (H)C(CC)-TOCSY-[^{15}N,^{1}H]-TROSY experiment at 800 MHz never matched the performance of the (H)C(CC)-TOCSY-(CO)-[^{15}N,^{1}H]-TROSY experiment measured at 500 MHz. For Val residues, the signal intensity was typically reduced two- to threefold in the 800 MHz (H)C(CC)-TOCSY-[^{15}N,^{1}H]-TROSY experiment when compared to the 500 MHz (H)C(CC)-TOCSY-(CO)-[^{15}N,^{1}H]-TROSY, and Leu and Ile residues yielded still lower relative intensity. Because of the extensive J value-related uncertainties of the predicted sensitivity (shadowed areas in Figure 4; the ranges for the experiment of Figure 6 are much wider because the transfer efficiencies are related to products of two coupling constants, as seen in Equations (A21) and (A22)), the experimental observations cannot really be considered to represent clear-cut discrepancies with the model calculations. The reduced signal intensity for the longer side chains nonetheless seems to indicate that imperfect TOCSY mixing may contribute to the apparent losses at higher field. In this work, DIPSI-3 mixing was used. Adiabatic mixing has been suggested as an alternative that might increase the sensitivity by 10–30% at 800 MHz (Peti et al., 2000). In the present experiments this would be only a marginal improvement, and therefore we chose to use the schemes of Figure 1.

Selection of the isotope labeling procedure

The labeling protocol proposed by Goto et al. (1999) has been applied because it provides selective protona-
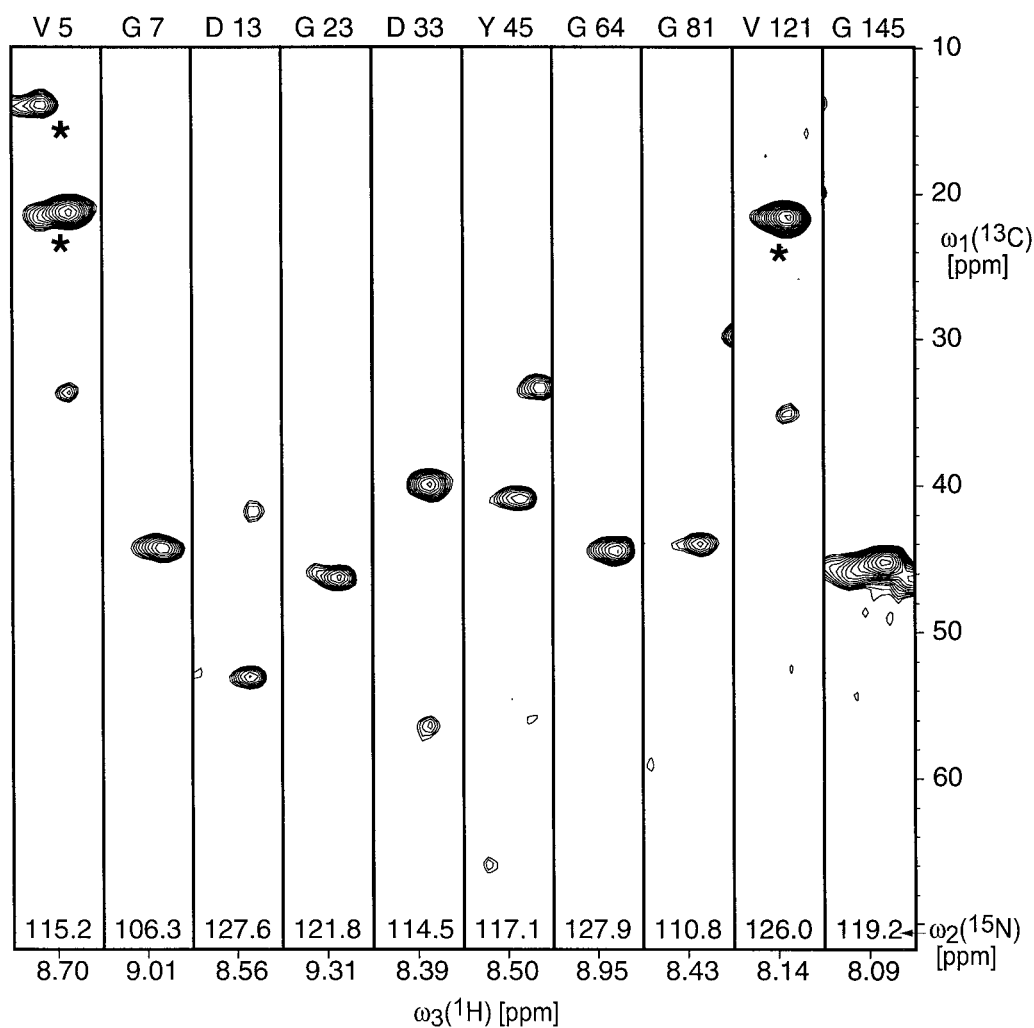
Figure 5. [ω_1(^{13}C), ω_3(^{1}H)]-strips from a 3D (H)C(CC)-TOCSY- (CO)-[^{15}N,^{1}H]-TROSY spectrum (digital spectral resolution 39 Hz (^{13}C), 12 Hz (^{15}N) and 8 Hz (^{1}H^N)). The strips cover the entire ^{13}C frequency range, and include peaks arising from steady-state ^{13}C magnetization (see text). Peaks originating from protonated methyl groups are marked with an asterisk (*).

tion of the Val-$\gamma^{1,2}$, Leu-$\delta^{1,2}$ and Ile-δ^1 methyl groups on a highly deuterated background. The fact that the CH$_n$ moieties separating the protonated methyl groups and the backbone amide groups are nearly completely depleted of protons enables one to record the NMR experiments described here with optimal efficiency of the magnetization transfer between the peripheral methyl groups and the backbone atoms. Compared to other possible approaches, there is also the advantage that no CH$_2$D and CHD$_2$ isotopomers are produced, and that high incorporation levels of protons are attained in the desired positions (Goto et al., 1999). Finally, the presently used protocol is also cost-effective, since the protein yield in *E. coli* cultures

grown on glucose as the carbon source is about two-fold higher than with pyruvate-based media (Gardner and Kay, 1998; Rosen et al., 1996).

Concluding remarks

Assignment of methyl groups from the combined use of TROSY-type NMR experiments and site-specific protonation on a highly deuterated background enables the collection of additional NOE restraints from ^{15}N- and ^{13}C-resolved 3D [^{1}H,^{1}H]-NOESY spectra. This data will improve the results of structure calculations of polypeptide chains for which extensive deuteration of all other positions is mandatory for ob-
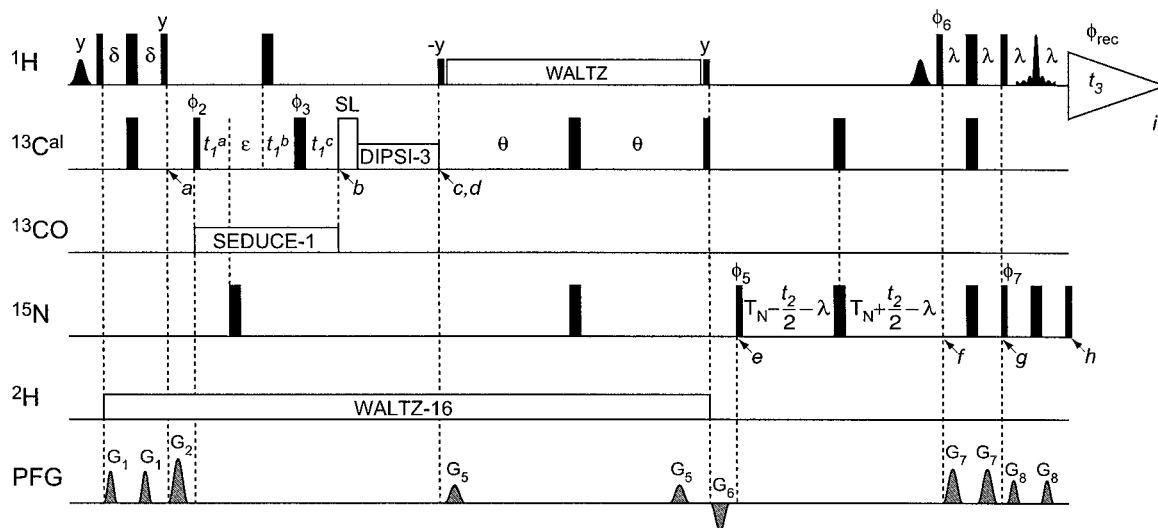
Figure 6. Pulse sequence of 3D (H)C(CC)-TOCSY-[^{15}N,^{1}H]-TROSY. All the parameters are identical to the (H)C(CC)-TOCSY-(CO)-[^{15}N,^{1}H]-TROSY scheme in Figure 1A, except for the following: $\theta = 13.2$ ms, duration of ^{13}C DIPSI-3 = 17.8 ms, the field strengths for the soft pulses were scaled with a factor of 8/5.

taining high-quality multidimensional NMR spectra. The availability of methyl–H^N and methyl–methyl distance constraints in addition to the backbone H^N–H^N NOEs can quite generally be expected to lead to significant improvement of the NMR structures of large molecules. In particular, for α-helical membrane proteins such NOEs may define the relative orientation of the individual helices. In this way, the presently described experiments may open avenues for structural studies of new classes of membrane proteins and possibly other large structures.

Appendix

This section presents the formalism used to compute the data in Figure 4. The descriptions of the parameters used are given in the legend to Figure 4. Relative signal intensities, S_{rel}, for the (H)C(CC)-TOCSY-(CO)-[^{15}N,^{1}H]-TROSY experiment were calculated as

$$S_{rel} = e^{-t_{cd} \cdot \delta_{C\alpha}^2 \cdot 4J(0)} \cdot \kappa_{cd} \cdot e^{-t_{de} \cdot \delta_{C'}^2 \cdot 4J(0)} \cdot \kappa_{de} \cdot$$
$$\frac{1}{\sqrt{2} R_s^H} \cdot e^{-t_{ef} \cdot R_s^N} \cdot r_{fh} \cdot \kappa_{eg}, \tag{A1}$$

and for the corresponding conventional experiment as

$$S_{rel} = e^{-t_{cd} \cdot \delta_{C\alpha}^2 \cdot 4J(0)} \cdot \kappa_{cd} \cdot e^{-t_{de} \cdot \delta_{C'}^2 \cdot 4J(0)} \cdot \kappa_{de} \cdot$$
$$\frac{1}{R_c^H} \cdot e^{-t_{ef} \cdot R_c^N} \cdot e^{-t_{fh} \cdot R_c^H} \cdot \kappa_{eg}. \tag{A2}$$

In this notation, c to i denote time points in Figure 1A. Relaxation rates for the TROSY step, from time point e in Figure 1 onwards, were calculated according to previous publications (Pervushin et al., 1997; Salzmann et al., 1998).

The interaction between CSA and dipole-dipole coupling gives rise to the following transverse relaxation rates of the four-line amide proton–nitrogen-15 multiplet:

$$R_s^N = \{p_{HN}^2 - (3\cos^2 \varphi_N - 1) p_{HN} \delta_N + \delta_N^2\} \cdot 4J(0)$$
$$+ \sum_i 2 p_{HK_i}^2 J(0) \tag{A3}$$

$$R_r^N = \{p_{HN}^2 + (3\cos^2 \varphi_N - 1) p_{HN} \delta_N + \delta_N^2\} \cdot 4J(0)$$
$$+ \sum_i 2 p_{HK_i}^2 J(0). \tag{A4}$$

R_s^N and R_r^N are the rates for the narrow and broad lines in the ^{15}N dimension, respectively. The corresponding rates for the two lines in the proton dimension are

$$R_s^H = \{p_{HN}^2 - (3\cos^2 \varphi_H - 1)p_{HN}\delta_H + \delta_H^2\} \cdot 4J(0)$$

$$+ \sum_i 5p_{HK_i}^2 J(0) \tag{A5}$$

$$R_r^H = \{p_{HN}^2 + (3\cos^2 \varphi_H - 1)p_{HN}\delta_H + \delta_H^2\} \cdot 4J(0)$$

$$+ \sum_i 5p_{HK_i}^2 J(0). \tag{A6}$$

Outside of the TROSY elements, the relaxation was calculated as

$$R_c^N = \frac{1}{2} \cdot (R_r^N + R_s^N) \tag{A7}$$

and

$$R_c^H = \frac{1}{2} \cdot (R_r^H + R_s^H). \tag{A8}$$

The dipolar interaction terms are

$$p_{HN} = -\frac{\mu_0}{4\pi} \cdot \frac{h}{4\pi\sqrt{2}} \cdot \frac{\gamma_H\gamma_N}{r_{HN}^3} \tag{A9}$$

and

$$p_{HK} = -\frac{\mu_0}{4\pi} \cdot \frac{h}{4\pi\sqrt{2}} \cdot \frac{\gamma_H^2}{r_{HK}^3}, \tag{A10}$$

and the CSA interaction terms are

$$\delta_H = \frac{1}{3\sqrt{2}}\gamma_H B_0 \Delta\sigma_H, \tag{A11}$$

$$\delta_N = \frac{1}{3\sqrt{2}}\gamma_N B_0 \Delta\sigma_N, \tag{A12}$$

$$\delta_{C'} = \frac{1}{3\sqrt{2}}\gamma_{C'} B_0 \Delta\sigma_{C'}, \tag{A13}$$

and

$$\delta_{C\alpha} = \frac{1}{3\sqrt{2}}\gamma_{C\alpha} B_0 \Delta\sigma_{C\alpha}. \tag{A14}$$

The following factors for through-bond transfer were used:

$$\kappa_{cd} = \sin \pi^1 J(C^\alpha, C')t_{cd} \tag{A15}$$

$$\kappa_{de} = \sin \pi^1 J(C', N)t_{de} \tag{A16}$$

$$\kappa_{eg} = \sin \pi^1 J(C', N)t_{eg} \tag{A17}$$

Finally, relaxation of single- and double-quantum coherences during the ST2-PT element between the time points f and h is taken into account with the factor

$$r_{fh} = \frac{1}{2} \left(e^{-t_{fh}/2 \cdot (R_c^N + \delta_H^2 \cdot 4J(0) + \delta_N^2 \cdot 4J(0))} + \right.$$
$$\left. e^{-t_{fh}/2 \cdot (R_c^H + \delta_H^2 \cdot 4J(0) + \delta_N^2 \cdot 4J(0))} \right). \tag{A18}$$

For the alternative (H)C(CC)-TOCSY-[^{15}N,^{1}H]-TROSY experiment (Figure 6), the relative signal intensities are

$$S_{rel} = e^{-t_{de} \cdot \delta_{C\alpha}^2 \cdot 4J(0)} \cdot \kappa_{de} \cdot \frac{1}{\sqrt{2}R_s^H} \cdot e^{-t_{ef} \cdot R_s^N} \cdot r_{fh} \cdot \kappa_{eg}, \tag{A19}$$

and for the corresponding conventional experiment we have

$$S_{rel} = e^{-t_{de} \cdot \delta_{C\alpha}^2 \cdot 4J(0)} \cdot \kappa_{de} \cdot \frac{1}{R_c^H} \cdot e^{-t_{ef} \cdot R_c^N} \cdot e^{-t_{fh} \cdot R_c^H} \cdot \kappa_{eg}, \tag{A20}$$

where

$$\kappa_{de} = \sin \pi^2 J(C^\alpha, N)t_{de} \cdot \cos \pi^1 J(N, C^\alpha)t_{de} \tag{A21}$$

and

$$\kappa_{eg} = \sin \pi^2 J(C^\alpha, N)t_{eg} \cdot \cos \pi^1 J(N, C^\alpha)t_{eg}, \tag{A22}$$

with $^2J(C^\alpha,N)$ and $^1J(N,C^\alpha)$ being the intraresidual and sequential coupling constants, respectively.

In all computations slowly tumbling molecules were assumed, and only terms containing the spectral density at zero frequency, $J(0)$, were taken into account. This simplification is valid as long as $\omega\tau_c \gg 1$, as is the case for high fields and large molecules (Pervushin et al., 1997).

In the equations (A1), (A2), (A19) and (A20), the terms $\frac{1}{R_s^H}$ and $\frac{1}{R_c^H}$ take account of relaxation during the acquisition period, so that the intensity of the resonance lines can be used directly for comparative studies. The factor $\sqrt{2}$ in equations (A1) and (A19) accounts for the increase in noise due to the addition of two independent traces in the TROSY experiment (Pervushin et al., 1998). The calculations were done for a perdeuterated β-sheet protein with a rotational correlation time of $\tau_c = 21$ ns (corresponding to $M_r = 60$ kDa), which mimics the behavior of OmpX/DHPC. The values used for the different parameters are listed in the legend to Figure 4.

References

Arora, A., Abildgaard, F., Bushweller, J.H. and Tamm, L.K. (2001) *Nat. Struct. Biol.*, **8**, 334–338.

Bax, A., Clore, G.M. and Gronenborn, A.M. (1990) *J. Magn. Reson.*, **88**, 425–431.

Bodenhausen, G. and Ruben, D.J. (1980) *Chem. Phys. Lett.*, **69**, 185–189.

Fernández, C., Adeishvili, K. and Wüthrich, K. (2001a) *Proc. Natl. Acad. Sci. USA*, **98**, 2358–2363.

Fernández, C., Hilty, C., Bonjour, S., Adeishvili, K., Pervushin, K. and Wüthrich, K. (2001b) *FEBS Lett.*, **504**, 173–178.

Gardner, K.H. and Kay, L.E. (1998) *Annu. Rev. Biophys. Biomol. Struct.*, **27**, 357–406.

Gardner, K.H., Konrat, R., Rosen, M.K. and Kay, L.E. (1996) *J. Biomol. NMR*, **8**, 351–356.

Geen, H. and Freeman, R. (1991) *J. Magn. Reson.*, **93**, 93–141.

Goto, N.K., Gardner, K.H., Mueller, G.A., Willis, R.C. and Kay, L.E. (1999) *J. Biomol. NMR*, **13**, 369–374.

Grzesiek, S., Anglister, J. and Bax, A. (1993) *J. Magn. Reson. B*, **101**, 114–119.

Hochuli, M., Szyperski, T. and Wüthrich, K. (2000) *J. Biomol. NMR*, **17**, 33–42.

LeMaster, D.M. (1994) *Prog. NMR Spectrosc.*, **26**, 371–419.

Lin, Y.X. and Wagner, G. (1999) *J. Biomol. NMR*, **15**, 227–239.

Logan, T.M, Olejniczak, E.T., Xu, R.X. and Fesik, S.W. (1993) *J. Biomol. NMR*, **3**, 225–231.

Loria, J.P., Rance, M. and Palmer, A.G. (1999) *J. Magn. Reson.*, **141**, 180–184.

Lyons, B.A. and Montelione, G.T. (1993) *J. Magn. Reson. B*, **101**, 206–209.

Lyons, B.A., Tashiro, M., Cedergren, L., Nilsson, B. and Montelione, G.T. (1993) *Biochemistry*, **32**, 7839–7845.

Marion, D., Ikura, M., Tschudin, R. and Bax, A. (1989) *J. Magn. Reson.*, **85**, 393–399.

Markley, J.L., Bax, A., Arata, Y., Hilbers, C.W., Kaptein, R., Sykes, B.D., Wright, P.E. and Wüthrich, K. (1998) *J. Biomol. NMR*, **12**, 1–23.

McCoy, M.A. and Mueller, L. (1992) *J. Am. Chem. Soc.*, **114**, 2108–2112.

Montelione, G.T., Lyons, B.A., Emerson, S.D. and Tashiro, M. (1992) *J. Am. Chem. Soc.*, **114**, 10974–10975.

Neri, D., Otting, G. and Wüthrich, K. (1990) *Tetrahedron*, **46**, 3287–3296.

Permi, P. and Annila, A. (2001) *J. Biomol. NMR*, **20**, 127–133.

Pervushin, K. (2000) *Q. Rev. Biophys.*, **33**, 161–197.

Pervushin, K., Riek, R., Wider, G. and Wüthrich, K. (1997) *Proc. Natl. Acad. Sci. USA*, **94**, 12366–12371.

Pervushin, K., Wider, G. and Wüthrich, K. (1998) *J. Biomol. NMR*, **12**, 345–348.

Peti, W., Griesinger, C. and Bermel, W. (2000) *J. Biomol. NMR*, **18**, 199–205.

Piotto, M., Saudek, V. and Sklenar, V. (1992) *J. Biomol. NMR*, **2**, 661–665.

Riek, R., Pervushin, K. and Wüthrich, K. (2000) *Trends Biochem. Sci.*, **25**, 462–468.

Rosen, M.K., Gardner, K.H., Willis, R.C., Parris, W.E., Pawson, T. and Kay, L.E. (1996) *J. Mol. Biol.*, **263**, 627–636.

Salzmann, M., Pervushin, K., Wider, G., Senn, H. and Wüthrich, K. (1998) *Proc. Natl. Acad. Sci. USA*, **95**, 13585–13590.

Salzmann, M., Pervushin, K., Wider, G., Senn, H. and Wüthrich, K. (2000) *J. Am. Chem. Soc.*, **122**, 7543–7548.

Salzmann, M., Wider, G., Pervushin, K. and Wüthrich, K. (1999) *J. Biomol. NMR*, **15**, 181–184.

Shaka, A.J., Keeler, J., Frenkiel, T. and Freeman, R. (1983) *J. Magn. Reson.*, **52**, 335–338.

Shaka, A.J., Lee, C.J. and Pines, A. (1988) *J. Magn. Reson.*, **77**, 274–293.

Wider, G. (1998) *Prog. NMR Spectrosc.*, **32**, 193–275.

Wider, G. and Wüthrich, K. (1999) *Curr. Opin. Struct. Biol.*, **9**, 594–601.

Wüthrich, K. (1986) *NMR of Proteins and Nucleic Acids*, Wiley, New York.

Wüthrich, K. (1998) *Nat. Struct. Biol.*, **5**, 492–495.